Journal of Crystal Growth 652 (2025) 128054

Contents lists available at ScienceDirect

Journal of Crystal Growth

journal homepage: www.elsevier.com/locate/jcrysgro

Optical and structural characteristics of AlInN/GaN superlattices with varying AlInN fractions

Haotian Xue *, Elia Palmese, Ben J. Sekely, Dakota Gray-Boneker, Antonio Gonzalez, Daniel J. Rogers, Brian D. Little, Fred A. Kish, Jr, John F. Muth, Jonathan J. Wierer, Jr *

Department of Electrical and Computer Engineering, North Carolina State University, Raleigh, NC 27695, USA

ARTICLE INFO

Communicated by Hongping Zhao

ABSTRACT

Data on the growth and characterization of AlInN/GaN superlattices (SLs) with varying AlInN fractions are presented. The SLs are grown using metal–organic chemical vapor deposition (MOCVD) and have AlInN fractions (AlInN thickness/SL period thickness) from 1 to 0.125 to explore the required GaN thickness to achieve good surface morphology. The SLs with AlInN fractions between 0.992 and 0.645 exhibited well-defined atomic steps and minimal surface defects, while lower fractions resulted in rougher surfaces. The highest AlInN fraction sample (0.992) has less than a monolayer of GaN but exhibits excellent surface morphology comparable to lower fractions. Energy-dispersive X-ray spectroscopy analysis on the highest 0.922 AlInN fraction sample revealed the expected periodic Ga incorporation but also a quaternary composition throughout with a baseline amount of Ga. Spectroscopic ellipsometry measurements demonstrated that the SLs provide refractive index tunability between GaN and AlInN. The results show that SLs maintain a smooth surface morphology across a wide range of AlInN fractions, offering excellent design flexibility for device applications.

1. Introduction

AlInN is an intriguing part of the AlInGaN alloy system because it has a lattice-matched condition to GaN with a wider bandgap [1]. It is used in waveguides and distributed Bragg reflectors [2–7], high-electron-mobility transistors (HEMTs) [8–10], and power devices [11,12], and it can be oxidized to create insulating layers for devices [13–15]. However, bulk AlInN suffers from columnar growth, surface mounding, and pit formation, even under the best-known conditions [16–18]. A recent solution to this problem is the growth of AlInN/GaN superlattices (SLs). SLs consisting of repeated pairs of 1 nm thick GaN and 3 nm thick AlInN can achieve smooth surface morphology that resembles the underlying GaN substrate or template layer [19]. This previous work showed growth conditions can affect morphology. For example, the SL surface roughens at pressures outside of 20 to 40 kPa and remains smooth with varying growth temperatures. Also, as the SLs become thicker, more precise lattice match conditions (and temperature control) are required to avoid relaxation and degraded surface morphologies.

Another important finding of Ref. [19] is the high refractive index contrast that can be achieved with the AlInN/GaN SL compared to GaN. The ability to customize the refractive index would be an essential tool for implementing AlInN/GaN SLs in optical devices. One could achieve index tunability if the AlInN fraction, defined as the thickness of the AlInN over the total SL period thickness, is varied. This potential and promising feature of AlInN/GaN SLs, refractive index tunability while maintaining lattice-matching and excellent surface morphology, is yet to be verified. Additionally, there is an open question on the limits of the AlInN fraction in the AlInN/GaN SL while keeping the superior morphology intact.

This work presents data on AlInN/GaN SLs with varying AlInN fractions grown by metal–organic chemical vapor deposition (MOCVD). The results show the SLs maintain a smooth surface morphology across a wide range of AlInN fractions. The sample set explores the required GaN thickness to achieve good surface morphology, and samples with AlInN fractions from 0.992 to 0.645 exhibited well-defined atomic steps and minimal surface defects, while lower fractions resulted in rougher surfaces. The highest AlInN fraction sample (0.992) has less than a monolayer of GaN but exhibits excellent surface morphology comparable to lower fractions. Energy-dispersive X-ray spectroscopy (EDS) analysis on the highest AlInN fraction sample revealed the expected periodic incorporation of Ga, as well as an overall quaternary composition with a small amount of Ga throughout. Spectroscopic ellipsometry (SE)

* Corresponding authors.
E-mail addresses: hxue8@ncsu.edu (H. Xue), jjwierer@ncsu.edu (J.J. Wierer, Jr).

https://doi.org/10.1016/j.jcrysgro.2025.128054
Received 26 November 2024; Received in revised form 2 January 2025; Accepted 4 January 2025
Available online 6 January 2025

measurements demonstrate the SLs provide refractive index tunability between GaN and AlInN, making them attractive for optical confinement layers in devices.

2. Experimental methods

The samples are grown by MOCVD in a Taiyo Nippon Sanso Co. (TNSC) SR2000 reactor on GaN-on-sapphire templates and GaN substrates with conditions similar to previous work [19]. The growth consists of a ~350 nm thick unintentionally doped GaN layer, AlInN/GaN SLs with a total thickness of ~75 nm, and a 2 nm thick GaN capping layer resulting from growth termination procedures. The growth pressure is 30 kPa, chosen from previous optimization studies [19]. All layers within the SLs are grown in an N_2 ambient with a V/III ratio of $\sim 1.44 \times 10^4$ and are unintentionally doped. The AlInN layers are grown with 10.6 μmol/min of TMAl and 9.5 μmol/min of TMIn, while the GaN layers are grown with 20 μmol/min of TEGa. The In content of the AlInN layers is nearly lattice-matched and varies from 0.11 to 0.18. Growth temperatures ranging from 785 °C to 815 °C were used. As shown in Ref. 19, the growth temperature change has minimal effect on the SL surface morphology compared to bulk AlInN layers.

Two sets of SL samples are grown, and a schematic cross-section is shown in Fig. 1. The AlInN fraction in the SLs is varied for each sample and is defined as

$$\text{AlInN Fraction} = \frac{t_{\text{AlInN}}}{t_{\text{AlInN}} + t_{\text{GaN}}} \quad (1)$$

where t_{AlInN} and t_{GaN} are the thickness of each layer. In the first set of samples, the SLs are grown on GaN-on-sapphire templates with AlInN fractions of 1, 0.992, 0.964, 0.927, 0.845, 0.75, 0.645, 0.25, and 0.125 by changing the AlInN and GaN thicknesses. The SLs have 20 periods with a constant period thickness of 3.5 nm. The second set of SL samples is grown on bulk GaN substrates to compare them to SLs on GaN-on-sapphire templates with higher dislocation densities. SLs with an AlInN fraction of 0.992 and 0.845 are grown in this set, with 20 periods and a period thickness of 3.5 nm. Information about the growth of the samples is listed in Table 1.

The morphology, composition, and thicknesses of the samples are characterized by X-ray diffraction (XRD), reciprocal space mapping (RSM), atomic force microscope (AFM), scanning transmission electron microscopy (STEM), and EDS. The optical properties are measured using SE and cathodoluminescence (CL). The details of these measurements and AlInN/GaN SLs are described previously [19].

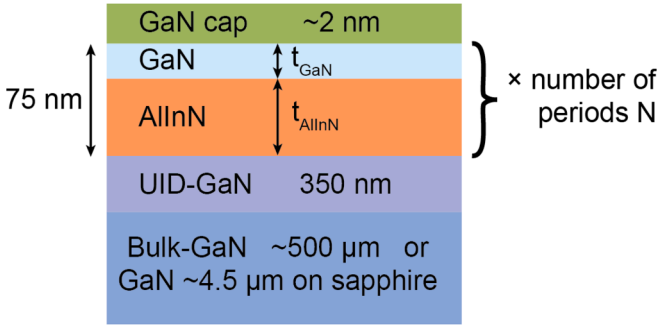

Fig. 1. Schematic cross-section of the AlInN/GaN superlattices (SL). The SLs consist of 20 periods with a constant period thickness of 3.5 nm for a total thickness of 75 nm. The AlInN fraction (AlInN thickness/total thickness) is varied, while the period thickness is the same. The samples in the first set are grown on GaN-on-sapphire substrates, while the second set is grown on bulk GaN substrates for comparison.

Table 1
Growth parameters and characteristic results for all samples.

ID	Shown in Figs	Substrate	AlInN Fraction	Growth Temperature (°C)	In (%)	AFM rms (nm)
M323	3(a)	GaN/Al_2O_3	1.000	790	15.8	0.62
M365	4(c)	GaN	0.845	815	13.7	0.13
M571	3(e)	GaN/Al_2O_3	0.845	810	12.4	0.29
M585	3(d), 6	GaN/Al_2O_3	0.927	810	13.6	0.24
M589	3(c), 6	GaN/Al_2O_3	0.964	810	12.1	0.29
M592	3(b), 4 (a), 6	GaN/Al_2O_3	0.992	810	11.2	0.24
M729	3(g), 6	GaN/Al_2O_3	0.645	785	18.0	0.28
M733	3(f)	GaN/Al_2O_3	0.750	785	17.5	0.32
M736	3(h), 6	GaN/Al_2O_3	0.250	785	18.0	0.50
M897	3(i)	GaN/Al_2O_3	0.125	785	18.0	0.62
M750	4(b), 5 (a, b)	GaN	0.992	810	15.0	0.15

3. Results and discussion

To verify the strain state of the SLs, X-ray RSM along the $(10\bar{1}5)$ reflection is performed on the sample with 0.845 AlInN fraction on a GaN-on-sapphire template. As shown in Fig. 2, the superlattice peak aligns with the GaN peak vertically, indicating the SL is pseudomorphic to the underlying GaN. It is assumed that all the SLs that exhibit excellent surface morphology are pseudomorphic since they lack the defects and surface roughness found in relaxed III-nitride films.

The impact on surface morphology versus the fraction of the AlInN in the SL is studied. Fig. 3 shows the SL samples with AlInN fractions of 0.992, 0.964, 0.927, 0.845, 0.75, 0.645, 0.25, and 0.125. A bulk AlInN sample is included in the figure as a control. It suffers from island growth, where the surface is decorated with mounds that form along the atomic steps, which is typical for AlInN bulk films [18]. The samples

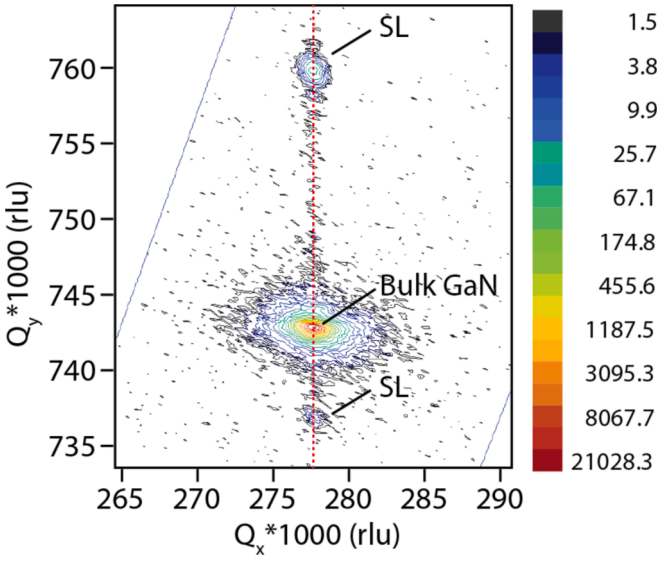

Fig. 2. X-ray reciprocal space map (RSM) of the $(10\bar{1}5)$ reflection for the sample with 0.845 AlInN fraction. The red line shows that the superlattice peak aligns with the GaN peak vertically, indicating the SL is pseudomorphic to GaN. (For interpretation of the references to colour in this figure legend, the reader is referred to the web version of this article.)

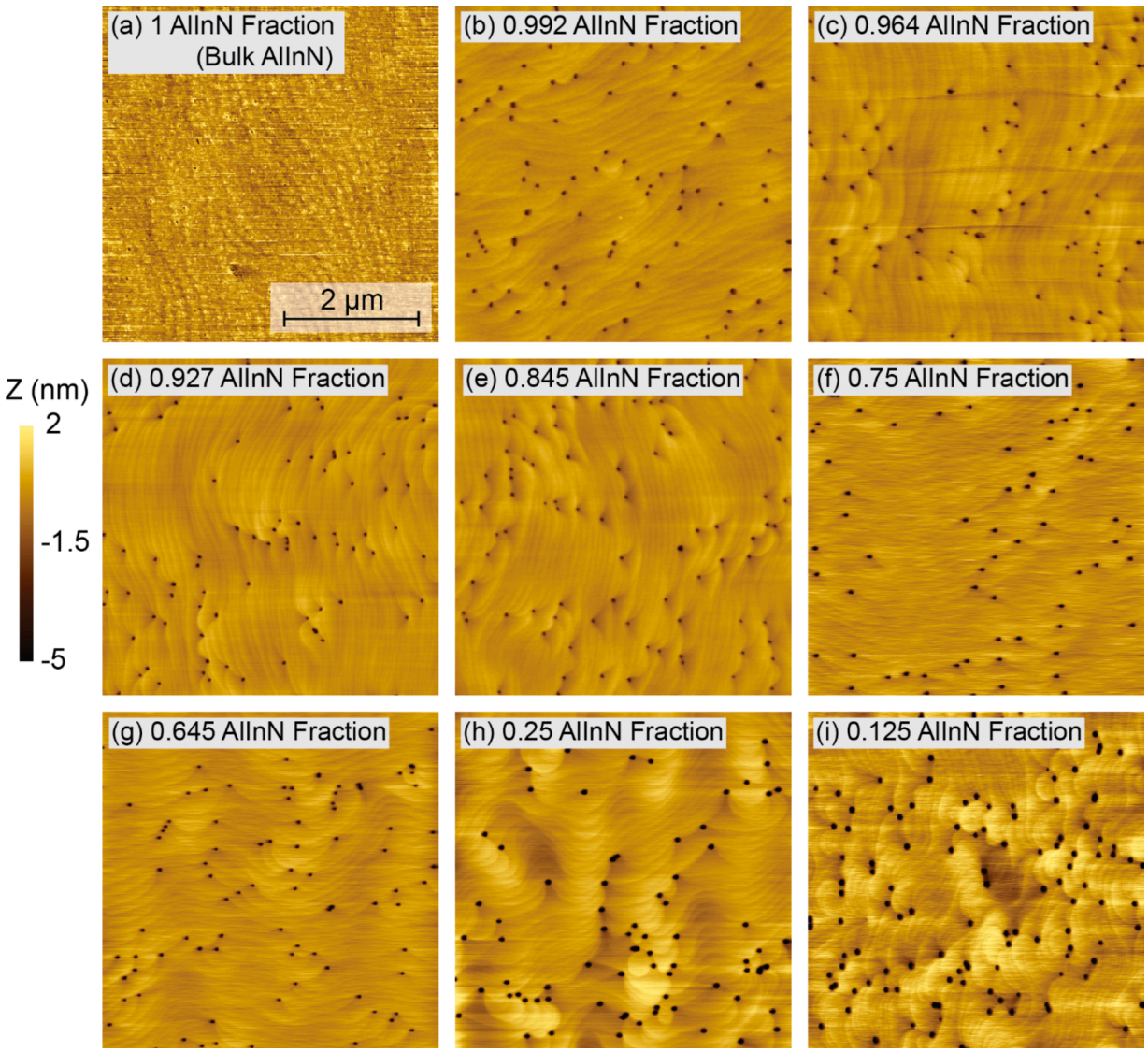

Fig. 3. Atomic force microscope (AFM) images of AlInN/GaN superlattices with the same period thickness and total thickness but varying AlInN fractions that are (a) 1 (bulk AlInN), (b) 0.992, (c) 0.964, (d) 0.927, (e) 0.845, (f) 0.75, (g) 0.645, (h) 0.25, and (i) 0.125. The AFM in (a) shows typical bulk AlInN surface morphology [19], and (b) through (g) show similar surface morphology with varying AlInN fractions. The AFMs in (h) and (i) show degrading surface morphology with decreasing AlInN fraction in the SL.

with AlInN fraction from 0.992 to 0.645 exhibit smooth surface morphologies with atomic steps and root mean square (rms) surface roughness of ~0.28 nm. Pits are present with size and density similar to the threading dislocation density (TDD) of the underlying GaN-on-sapphire substrate (~3×10^8 cm^{-2}). The samples with 0.25 and 0.125 AlInN fractions also show relatively smooth morphology, albeit with wavier surfaces (rms ~0.5 nm) and more prominent pits with similar density to the substrate. The percentage of the surface covered by pits is ~1.7 % for the sample with 0.25 AlInN fraction, and 2.3 % for the sample with 0.125 AlInN fraction, higher than the samples with AlInN fraction from 0.992 to 0.645, which is ~1 %. It is suspected that as the thickness of the GaN layers increases, the suboptimal growth temperature for GaN results in the rougher surface morphology observed. These results indicate that the SLs can retain excellent surface morphology with AlInN fractions ranging from very close to 1 to ~0.65.

Particular attention is drawn to the sample with a 0.992 duty cycle. It has a very high AlInN fraction, making it compositionally extremely close to bulk AlInN while retaining the characteristic smooth surface of the SLs. The same growth recipe is repeated on a bulk GaN substrate with very low etch pit density (<5×10^4 cm^{-2}) to remove the pit (TDD) density contribution from the GaN-on-sapphire substrate. Fig. 4 (a) and (b) show the SLs grown on a GaN-on-sapphire template and GaN substrate, respectively, with AlInN fractions of 0.992. The AlInN/GaN SL on the GaN substrate has an excellent surface with clearly visible atomic steps and no pits. The observed surface pits are most likely propagated from pits in the respective substrates during growth, where their densities are kept the same. Fig. 4(c) shows a sample with the same total thickness and periods but an AlInN fraction of 0.845 [19] as a comparison. More irregular atomic steps are observed with slightly wider steps and variable width in Fig. 4(b) but remain predominantly parallel and evenly spaced. The low pit densities and excellent surface morphology of these layers on GaN substrates show they are good candidate in optical devices that operate at high current densities such as laser diodes.

Cross-sectional STEM is performed on the sample presented in Fig. 4 (b), and the results are shown in Fig. 5. STEM was chosen for this sample to avoid the pits caused by threading dislocations when growing on GaN-on-sapphire templates. The faint white parallel lines indicate the Ga within the periodic SL structure. EDS reveals the periodicity of the changing Ga and Al compositions. Within every SL period, the Ga atomic

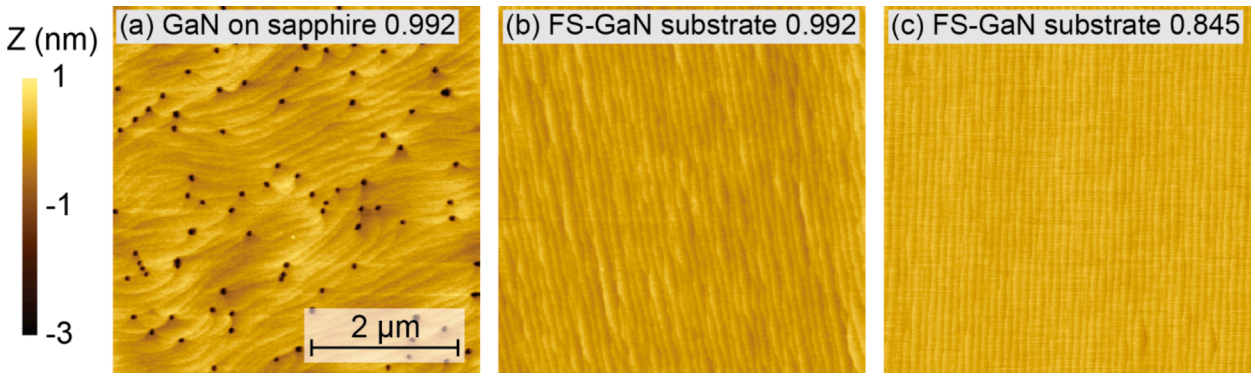

Fig. 4. Atomic force microscope (AFM) images of AlInN/GaN superlattices grown on (a) GaN-on-sapphire substrate with AlInN fraction of 0.992, (b) GaN substrate with AlInN fraction of 0.992, and (c) GaN substrate with AlInN fraction of 0.845 [19]. Both (a) and (b) have an AlInN fraction of 0.992, and (c) has an AlInN fraction of 0.845. Compared to (a), the AFM image in (b) shows a smooth surface with clear and parallel GaN atomic steps and no pits. The atomic steps in (b) are slightly wider and have variable widths compared to (c).

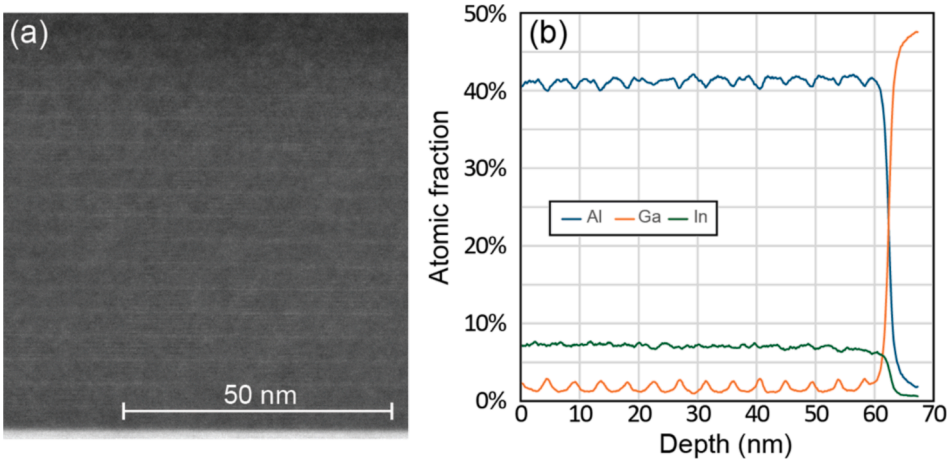

Fig. 5. (a) Cross-sectional STEM of the SL sample with 0.992 AlInN fraction grown on a bulk GaN substrate. Faint white lines are observed, indicating a periodic SL structure. (b) EDS line scan of the same sample. The Ga atomic fractions fluctuate periodically between ~0.013 to ~0.025 (out of 0.5 for Group III elements).

fraction rises from ~0.013 to ~0.025 (out of 0.5 for Group III elements). This is consistent with the AlInN fraction of 0.992 because the total thickness of GaN constitutes less than 1 % of the total period thickness and insufficient material is provided to grow a full monolayer of GaN. The EDS also suggests this SL structure is, in fact, a quaternary material throughout, with periodically varying Ga and Al composition. A background level of Ga content is observed to be around 0.025. This is potentially caused by the auto-incorporation of Ga from the surrounding chamber surfaces [20]. Overall, the layer shows a combined Ga composition of ~0.034. Most notably, the SL retained the smooth GaN-like surface morphology with an average composition of ~96.6 % AlInN. This shows that producing smooth surfaces takes only a fraction of a GaN layer in the SL.

One of the primary use cases for this structure is as an optical confinement layer. SE is performed to measure the refractive index for the samples with varying AlInN fractions. The result is plotted in Fig. 6 for light at 401, 501, and 601 nm. The x-axis is the AlInN fraction, which is adjusted with the background Ga level observed in EDS in Fig. 5(b). In general, the refractive index of the SL is a weighted average between AlInN and GaN. Some errors are caused by indium content variability from growth deviations since indium content is very sensitive to temperature fluctuations. Additionally, there is a steeper drop-off in the index at the higher AlInN fractions, which requires further study. This highlights the potential of the AlInN/GaN SL for optical devices as a layer that is conveniently tunable in refractive index while maintaining its surface morphology and lattice-matched crystal structure.

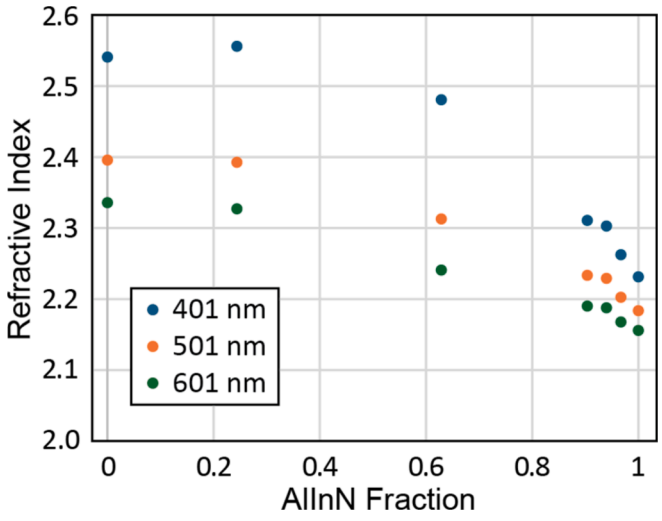

Fig. 6. Refractive index measured by spectroscopic ellipsometry (SE) for SL samples with varying AlInN fraction from 0 (bulk GaN) to 1 (bulk AlInN) at wavelengths of 401, 501, and 601 nm.

Cathodoluminescence (CL) is performed on samples with different GaN thicknesses to study the light emission from the GaN layers. An emission of ~312 nm is observed for the sample with ~0.27 nm of GaN layers, which is ~5 nm shorter than the ~317 nm emission observed in a structure with GaN layers twice as thick, similar to the one shown in Fig. 3(e). The spectral shapes are similar to those shown previously [19]. This indicates that as the GaN layer thickness is reduced, the light emission from the GaN layers does not blue-shift as significantly as expected for a rectangular quantum well. Combined with the evidence from the STEM results, it is evident that the interfaces between GaN and AlInN are intermixed, creating quantum wells with sloped barriers, which causes an increase in the quantum well bandgap.

4. Conclusion

AlInN/GaN SLs with varying AlInN fractions are presented. The surface morphology is excellent for a wide range of AlInN fractions and allows refractive index tuning. These results show that the AlInN/GaN SL is interesting for optical devices as a layer to conveniently tune the refractive index while maintaining its surface morphology and lattice-matched crystal structure.

CRediT authorship contribution statement

Haotian Xue: Writing – review & editing, Writing – original draft, Visualization, Validation, Software, Resources, Methodology, Investigation, Formal analysis, Data curation, Conceptualization. **Elia Palmese:** Writing – review & editing, Validation, Methodology, Investigation, Data curation, Conceptualization. **Ben J. Sekely:** Writing – review & editing, Validation, Resources, Methodology, Investigation, Formal analysis, Data curation. **Dakota Gray-Boneker:** Writing – review & editing, Methodology, Investigation, Data curation. **Antonio Gonzalez:** Writing – review & editing, Investigation, Data curation. **Daniel J. Rogers:** Writing – review & editing, Validation, Software, Methodology, Investigation, Formal analysis, Data curation. **Brian D. Little:** Writing – review & editing, Resources, Project administration, Data curation. **Fred A. Kish Jr:** Writing – review & editing, Supervision, Resources, Funding acquisition. **John F. Muth:** Writing – review & editing, Supervision, Resources, Investigation, Funding acquisition. **Jonathan J. Wierer Jr:** Writing – review & editing, Supervision, Resources, Project administration, Methodology, Investigation, Funding acquisition, Formal analysis, Data curation, Conceptualization.

Declaration of competing interest

The authors declare that they have no known competing financial interests or personal relationships that could have appeared to influence the work reported in this paper.

Acknowledgments

JJW, HX, and EP acknowledge funding from the U.S. National Science Foundation (Award numbers 1935295 and 2212639). We gratefully thank Christopher Winkler, and Roberto Garcia at NC State University for their assistance in STEM measurements. We thank TNSC for their support with the MOCVD growth.

This work was performed in part at both the NCSU Nanofabrication Facility (NNF) and the Analytical Instrumentation Facility (AIF) at North Carolina State University. Both facilities are members of the North Carolina Research Triangle Nanotechnology Network (RTNN), a site in the National Nanotechnology Coordinated Infrastructure (NNCI) supported by the National Science Foundation (Grant No. ECCS-1542015 and ECCS-2025064).

Data availability

Data will be made available on request.

References

[1] S. Yamaguchi, et al., Structural and optical properties of AlInN and AlGaInN on GaN grown by metalorganic vapor phase epitaxy, *J. Cryst. Growth* 195 (1–4) (1998) 309–313.
[2] J.F. Carlin, et al., Progresses in III-nitride distributed Bragg reflectors and microcavities using AlInN/GaN materials, *Physica Status Solidi B-Basic Solid State Physics* 242 (11) (2005) 2326–2344.
[3] S. Yoshida *et al.*, "Electron and hole accumulations at GaN/AlInN/GaN interfaces and conductive n-type AlInN/GaN distributed Bragg reflectors," *Japanese Journal of Applied Physics,* vol. 55, no. 5, 2016.
[4] K. Arakawa *et al.*, "450 nm GaInN ridge stripe laser diodes with AlInN/AlGaN multiple cladding layers," *Japanese Journal of Applied Physics,* vol. 58, no. SC, 2019.
[5] M. Malinverni *et al.*, "InAlN cladding implementation in green superluminescent diodes and lasers," *Applied Physics Letters,* vol. 122, no. 20, 2023.
[6] M. Malinverni, et al., Blue and Green Low Threshold Laser Diodes With InAlN Claddings, *IEEE Photon. Technol. Lett.* 35 (24) (2023) 1303–1306.
[7] K. Kobayashi *et al.*, "N-type conducting AlInN/GaN distributed Bragg reflectors with AlGaN graded layers," *Japanese Journal of Applied Physics,* vol. 62, no. Sn, 2023.
[8] C. Gaquiere, et al., "AlInN/GaN a suitable HEMT device for extremely high power high frequency applications," in, *IEEE/MTT-S International Microwave Symposium* 2007 (2007) 2145–2148.
[9] M. Gonschorek, J. F. Carlin, E. Feltin, M. A. Py, and N. Grandjean, "High electron mobility lattice-matched AlInN/GaN field-effect transistor heterostructures," *Applied Physics Letters,* vol. 89, no. 6, 2006.
[10] E. Palmese, H. Xue, S. Pavlidis, J.J. Wierer, Enhancement-Mode AlInN/GaN High-Electron-Mobility Transistors Enabled by Thermally Oxidized Gates, *IEEE Trans. Electron Devices* 71 (2) (2024) 1003–1009.
[11] M.R. Peart, N. Tansu, J.J. Wierer, AlInN for Vertical Power Electronic Devices, *IEEE Trans. Electron Devices* 65 (10) (2018) 4276–4281.
[12] M.R. Peart, D. Borovac, W. Sun, R.B. Song, N. Tansu, J.J. Wierer, AlInN/GaN diodes for power electronic devices, *Appl. Phys Express* 13 (9) (2020) 091006.
[13] M.R. Peart, X.L. Wei, D. Borovac, W. Sun, N. Tansu, J.J. Wierer, Thermal Oxidation of AlInN for III-Nitride Electronic and Optoelectronic Devices, *ACS Appl. Electron. Mater.* 1 (8) (2019) 1367–1371.
[14] E. Palmese, H. Xue, R. Song, and J. J. Wierer, "Thermal oxidation of lattice mismatched Al1-xInxN films on GaN," *e-Prime - Advances in Electrical Engineering, Electronics and Energy,* vol. 5, 2023.
[15] E. Palmese, M.R. Peart, D. Borovac, R. Song, N. Tansu, J.J. Wierer, Thermal oxidation rates and resulting optical constants of Al0.83In0.17N films grown on GaN, *J. Appl. Phys.* 129 (12) (2021) 125105.
[16] R.B. Chung, et al., Growth study and impurity characterization of Al InN grown by metal organic chemical vapor deposition, *J. Cryst. Growth* 324 (1) (2011) 163–167.
[17] D. Borovac, W. Sun, R.B. Song, J.J. Wierer, N. Tansu, On the thermal stability of nearly lattice-matched AlInN films grown on GaN via MOVPE, *J. Cryst. Growth* 533 (2020) 125469.
[18] H. Xue, E. Palmese, R. Song, M. I. Chowdhury, N. C. Strandwitz, and J. J. Wierer, "Structural and optical characterization of thin AlInN films on c-plane GaN substrates," *Journal of Applied Physics,* vol. 134, no. 7, 2023.
[19] H. Xue, et al., Growth and characterization of AlInN/GaN superlattices, *J. Cryst. Growth* 630 (2024).
[20] J. Kim, et al., Origins of unintentional incorporation of gallium in InAlN layers during epitaxial growth, part II: Effects of underlying layers and growth chamber conditions, *J. Cryst. Growth* 388 (2014) 143–149.